Journal
ofOrgano
metallic
Chemistry

ELSEVIER

Synthesis, spectroscopy, and structural characterization of carbonyl and cage phosphite adducts of edge-bridged open metallocenes

Vichien Kulsomphob [a,b], Robert Tomaszewski [a,b], Arnold L. Rheingold [b], Atta M. Arif [a,b], Richard D. Ernst [a,*]

[a] *Department of Chemistry, University of Utah, 315 South 1400 East, Salt Lake City, UT 84112-0850, USA*
[b] *Department of Chemistry, University of Delaware, Newark, DE 19716, USA*
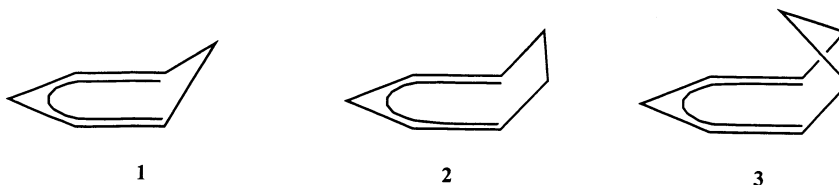
Abstract

The bis(cyclooctadienyl) complexes of titanium and vanadium form mono(ligand) adducts with both CO and cage phosphites. The 16 electron titanium complexes are diamagnetic, and the broadness of the ^{1}H-NMR chemical shifts for the phosphite complex indicates rapid, reversible ligand dissociation. The various complexes have been characterized analytically, through IR, NMR, and ESR spectroscopies, and X-ray diffraction. Structural data reveal a high degree of steric crowding in these species, while IR data for the carbonyl complexes reveal that these edge-bridged dienyl ligands are substantially better electron donors than typical pentadienyl ligands, even being quite comparable to C_5H_5. © 2002 Elsevier Science B.V. All rights reserved.

Keywords: Metal carbonyl; Open metallocene; Cyclooctadienyl complex

1. Introduction

While a substantial understanding of both the electronic and steric properties of pentadienyl ligands has been gained [1], much remains to be understood about how these properties are affected by the presence of edge-bridges, such as in cyclohexadienyl (**1**), cycloheptadienyl (**2**), or cyclooctadienyl (**3**) ligands. This is in some sense ironic, given that edge-bridged open ferrocenes ('pseudo-ferrocenes', e.g. **4** [2]) were reported earlier than the simple open ferrocenes themselves (e.g. **5** [3]). Wolczanski et al. have reported a series of bis(6,6-dimethylcyclohexadienyl)metal complexes, M(6,6-dmch)₂, for M = Ti, V, Cr, Fe, and possibly Mn, and found that the properties of the edge-bridged 6,6-dmch ligand (**6**) differ substantially from those of other

1   **2**   **3**

pentadienyl ligands [4], appearing to be sterically more demanding, with electronic properties intermediate between those of C_5H_5 and simple pentadienyl ligands.

* Corresponding author. Tel.: +1-801-581-6681; fax: +1-801-581-8433.
E-mail address: ernst@chemistry.utah.edu (R.D. Ernst).

4   **5**

6
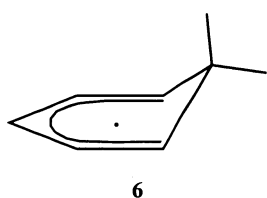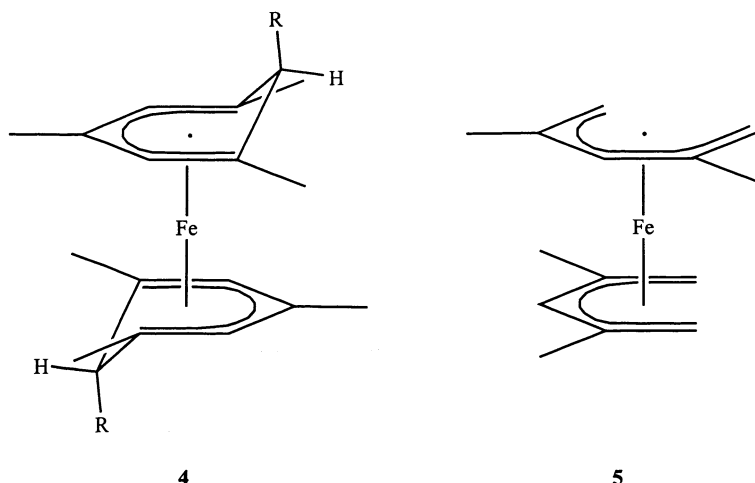
A subsequent report of an analogous series of M(c-C_8H_{11})$_2$ (c-C_8H_{11} = cyclooctadienyl; M = Ti, V, Cr, Fe) complexes, including their structural characterizations, provided additional insight into the edge-bridged dienyl ligands [5]. In particular, comparisons between the M(6,6-dmch)$_2$ and M(c-C_8H_{11})$_2$ complexes revealed that changes in the edge-bridge could have significant effects on the natures of their metal complexes. Here we report on the syntheses and characterizations of Lewis base adducts of the M(c-C_8H_{11})$_2$ (M = Ti, V) complexes. Such species are amenable to IR and ESR spectroscopic studies, which taken together with structural data, can provide additional information concerning the effects brought about by dienyl edge-bridges, whether relative to other edge-bridged species or to non-bridged ligands.

2. Experimental

All preparations, reactions, and manipulations of these compounds were carried out under a prepurified nitrogen atmosphere, using either Schlenk techniques or a glovebox. Hydrocarbon, ethereal, and aromatic solvents were dried and deoxygenated by distillation from sodium benzophenone ketyl under a nitrogen atmosphere. Spectroscopic data were obtained as previously described [6]. The ^{13}C-NMR spectra were not precisely integrated, but numbers of carbon atoms are reported in accord with their assignments. Elemental analyses were obtained from E&R Microanalytical Labs, Robertson Microanalytical Labs, or Desert Analytics. Ti(c-C_8H_{11})$_2$ and V(c-C_8H_{11})$_2$ were prepared as previously described [5], while the cage phosphite (caution: toxic) was obtained commercially.

2.1. Ti(c-C_8H_{11})$_2$[P(OCH$_2$)$_3$CC$_2$H$_5$]

A 250 ml, 2-neck flask equipped with a magnetic stirring bar and nitrogen inlet was charged with Ti(η^5-C_8H_{11})$_2$ (0.91 g, 3.5 mmol) in 50 ml of ether. The green solution was cooled to −78 °C and the 'cage phosphite', P(OCH$_2$)$_3$CC$_2$H$_5$ (0.62 g, 3.8 mmol, 1.1 equivalents) was added, at which time the solution turned orange. The reaction mixture was warmed to room temperature (r.t.). The solvent was then removed in vacuo leaving behind an orange–yellow solid. The residue was extracted into two 50 ml portions of ether and filtered through a Celite pad on a coarse frit. Concentration in vacuo of the orange filtrate to ca. 20 ml and placement into a −30 °C freezer gave 1.2 g (86%) of the complex as air-sensitive yellow cube-shaped crystals (m.p. 78–80 °C).

Anal. Calcd. for C$_{22}$H$_{33}$PO$_3$Ti: C, 62.21; H, 7.84. Found: C, 62.20; H, 8.01%. ^{1}H-NMR (toluene-d_8, −20 °C): δ 5.72 (t, 2H, J = 9.0 Hz, H-3), 3.91 (t, 4H, J = 11.0 Hz, H-2,4), 3.71 (d, 6H, J = 4.1 Hz, P(OCH$_2$)$_3$), 2.79 (t, 4H, J = 13.2 Hz, H-1,5), 2.51 (m, 8H, H-6,8), 1.40 (d, 2H, J = 13.7 Hz, H-7), 0.88 (q, 2H, J = 13.7 Hz, H-7′), 0.34 (q, 2H, J = 7.5 Hz, CH$_2$CH$_3$), 0.20 (t, 3H, J = 7.2 Hz, CH$_2$CH$_3$).

^{13}C-NMR (toluene-d_8, −20 °C): δ 119.7 (dt, 2C, J = 160, 9 Hz, C-3), 105.1 (dt, 4C, J = 156, 9 Hz, C-2,4), 72.6

(td, 3C, $J = 146$ Hz, $J_{C-P} = 6$ Hz, P(OCH$_2$)$_3$CCH$_2$–CH$_3$), 69.2 (d, 4C, $J = 145$ Hz, C-1,5), 34.0 (d, 1C, $J_{C-P} = 27$ Hz, P(OCH$_2$)$_3$CCH$_2$CH$_3$), 30.1 (t, 4C, $J = 128$ Hz, C-6,8), 23.6 (t, 2C, $J = 129$ Hz, C-7), 21.5 (t, 1C, $J = 123$ Hz, CH$_2$CH$_3$), 7.0 (q, 1C, $J = 126$ Hz, CH$_2$CH$_3$).

Mass spectrum (EI, 70 eV) m/z (relative intensity): 420 (14), 263 (21), 262 (52), 261 (23), 260 (66), 259 (42), 258 (77), 257 (17), 256 (10), 231 (21), 230 (44), 229 (21), 216 (12), 203 (10), 164 (8), 163 (100), 162 (8), 132 (25), 81 (14), 69 (14), 68 (22), 67 (21), 41 (11).

2.2. $V(c\text{-}C_8H_{11})_2(CO)$

Over a green solution of V(c-C$_8$H$_{11}$)$_2$ (1.00 g, 3.77 mmol) in 20 ml pentane under nitrogen was passed a stream of CO at -78 °C. After 10 min a distinct color change to a red solution had occurred. The reaction mixture was warmed to r.t. and the solvent removed in vacuo to give a red solid. The red residue was extracted into two 50 ml portions of pentane and filtered through a Celite pad on a coarse frit. The red filtrate was concentrated to 20 ml and cooled to -90 °C, giving a red crystalline product (0.81 g, 90% yield, m.p. 110 °C (dec.)).

Anal. Calcd. for C$_{17}$H$_{22}$OV: C, 69.62; H, 7.56. Found: C, 69.85; H, 7.56%. EPR (hexane, 20 °C): $g = 1.986$; $A_v = 76.6$ G. IR (Nujol mull): 1870 cm^{-1} (CO).

Mass spectrum (EI, 17 eV) m/z (relative intensity): 293 (49), 265 (29), 261 (53), 260 (25), 259 (100), 258 (26), 257 (26), 232 (16), 231 (53), 218 (15), 155 (69), 153 (72), 129 (84), 116 (56), 51 (21).

2.3. $V(c\text{-}C_8H_{11})_2[P(OCH_2)_3CEt]$

A 250 ml, 2-neck flask equipped with a magnetic stirring bar and nitrogen inlet was charged with V(c-C$_8$H$_{11}$)$_2$ (1.00 g, 3.77 mmol) in 50 ml of ether. The green solution was cooled to -78 °C and the 'cage phosphite', P(OCH$_2$)$_3$CEt (0.62 g, 3.8 mmol, 1.1 equivalents) was added at which time the solution turned lighter green. The reaction mixture was warmed to r.t. after which time the lighter green solution remained. Then the solvent was removed in vacuo leaving behind a green solid. The residue was extracted into two 50 ml portions of ether and filtered through a Celite pad on a coarse frit. The green filtrate was concentrated to 20 ml and cooled to -30 °C, giving a green crystalline product (1.23 g, 85% yield, m.p. 85–87 °C).

Anal. Calcd. for C$_{22}$H$_{33}$PO$_3$V: C, 61.82; H, 7.78. Found: C, 61.66; H, 7.83%. EPR (hexane, 20 °C): $g = 1.985$; $A_v = 76.6$ G; $A_P = 32.1$ G. Mass spectrum (EI, 17 eV) m/z (relative intensity): 265 (45), 261 (44), 260 (25), 259 (52), 258 (32), 257 (26), 232 (19), 231 (62), 218 (19), 162 (57), 155 (61), 153 (68), 132 (100), 129 (76), 117 (20), 116 (41), 109 (28), 69 (30), 68 (70), 67 (31), 51 (13), 41 (33).

Table 1
Crystal data and refinement parameters for Ti(c-C$_8$H$_{11}$)$_2$[P(OCH$_2$)$_3$CC$_2$H$_5$], V(c-C$_8$H$_{11}$)$_2$(CO), and V(c-C$_8$H$_{11}$)$_2$[P(OCH$_2$)$_3$CEt]

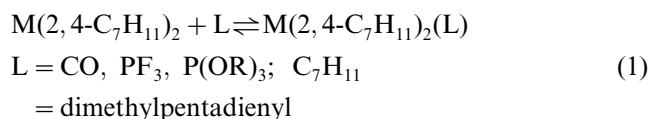| Formula	TiPO$_4$C$_{26}$H$_{43}$	VOC$_{17}$H$_{22}$	VPO$_3$C$_{22}$H$_{33}$
Formula weight	498.50	293.29	427.39
Temperature (K)	198	298	298
λ (Å)	0.71073	0.71073	0.71073
Crystal system	Triclinic	Monoclinic	Triclinic
Space group	$P\bar{1}$	$P2_1/m$	$P\bar{1}$
Unit cell dimensions			
a (Å)	9.447(2)	6.9739(4)	12.282(2)
b (Å)	11.452(4)	16.058(2)	13.229(2)
c (Å)	12.413(3)	7.0405(5)	14.922(2)
α (°)	91.17(2)	90	111.72(1)
β (°)	110.62(2)	115.828(8)	97.15(2)
γ (°)	91.39(2)	90	109.27(2)
Volume (Å^3); Z	1256.0;2	709.7(2); 2	2040.4;4
Density (calc)	1.325	1.372	1.391
Absorption coefficient (cm^{-1})	4.29	6.88	5.84
θ Range	1–24°	3.2–30	2–21.5
Limiting indices	+10; −12, 13; −13, 12	−1, 9; −1, 22; ±9	-1,12;-12,11;±15
Reflections collected	4215	2774	5226
Independent reflections; n: $I > n\sigma(I)$	3447; 3	2126;2	4439;2
$R(F)$	0.0472	0.0354	0.0453
$R(wF^2)$	0.0510	0.0821	0.1047
Maximum difference Fourier peak (e Å^{-3})	0.55	0.27	0.32

2.4. Crystallographic structural determinations

Crystal, data collection, and refinement parameters are given in Table 1. Suitable crystals were selected and mounted in thin-walled, nitrogen-flushed, glass capillaries. Each structure was solved by direct methods and subsequent difference Fourier syntheses and least-squares refinements. Most hydrogen atoms were treated as idealized contributions, except for those attached to the metal-bound carbon atoms of the open dienyl ligand in the titanium complex. All non-hydrogen atoms were refined anisotropically. The systematic absences in the diffraction data were consistent with the reported space groups. The vanadium carbonyl compound was found to be isomorphous with its titanium analogue [5]. One ether solvent molecule cocrystallized with the titanium complex, while for the vanadium phosphite complex there were two crystallographically independent, but otherwise similar, molecules present in the lattice. All software and sources of the scattering factors are contained in the SHELXTL (5.3) program library (G. Sheldrick, Siemens XRD, Madison, WI).

3. Results and discussion

A fairly common reaction of open titanocenes and open vanadocenes is the formation of 16 and 17 electron mono(ligand) adducts (Eq. (1) [7]).
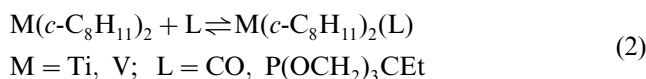
In the

$$M(2,4\text{-}C_7H_{11})_2 + L \rightleftharpoons M(2,4\text{-}C_7H_{11})_2(L)$$
$$L = CO, PF_3, P(OR)_3; \quad C_7H_{11} \qquad (1)$$
$$= \text{dimethylpentadienyl}$$

case of the titanium complexes, the actual ΔH and ΔS values for the coordination equilibria have been measured, and are consistent with the observation of strong binding at room temperature by PF_3, $P(OCH_2)_3CR$, and PMe_3, and progressively weaker binding by regular phosphites and PEt_3 [8]. In contrast to the strong binding of $Ti(2,4\text{-}C_7H_{11})_2$ by PMe_3, it is notable that significant coordination of $Ti(c\text{-}C_8H_{11})_2$ ($c\text{-}C_8H_{11} = $ cyclooctadienyl) by PMe_3 requires cooling to below -40 °C, although strong coordination does occur for CO [5]. Quite similar observations have been reported for $Ti(6,6\text{-}dmch)_2$ (dmch = dimethylcyclohexadienyl) [4]. The weaker binding of additional ligands by these complexes, compared with their $M(2,4\text{-}C_7H_{11})_2$ analogues, can easily be attributed to the presence of the edge-bridges. Thus, while Lewis base coordination in simple open [9] and half-open [10] metallocenes takes place by the open dienyl edges, as in **7**, the presence of an edge-bridge in a half-open


7   **8**
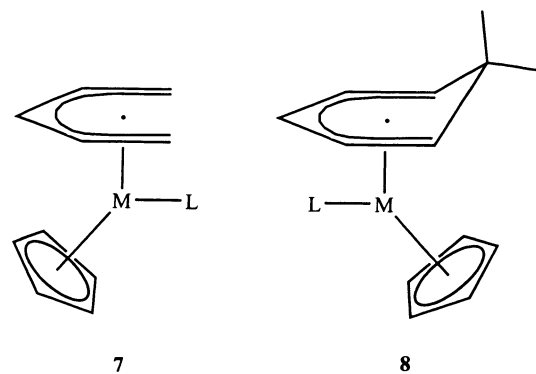
metallocene leads to coordination at the opposite end of the dienyl ligand, as in **8** [11].

Given the weak binding of PMe_3 to the $M(c\text{-}C_8H_{11})_2$ complexes of titanium and vanadium [5,12], it was of interest to see if strong coordination could be realized for some other phosphorus donor ligand. Indeed, addition of the cage phosphite, $P(OCH_2)_3CEt$, to solutions of either $M(c\text{-}C_8H_{11})_2$ complex led to an immediate color change, indicative of the formation of the appropriate adducts. Furthermore, $V(c\text{-}C_8H_{11})_2$ was found to form a carbonyl adduct, analogous to the reported $Ti(c\text{-}C_8H_{11})_2(CO)$ (Eq. (2)). Each of the carbonyl

$$M(c\text{-}C_8H_{11})_2 + L \rightleftharpoons M(c\text{-}C_8H_{11})_2(L)$$
$$M = Ti, V; \quad L = CO, P(OCH_2)_3CEt \qquad (2)$$

complexes displayed a single C–O stretch in the infrared spectra (1870 vs. 1879 cm^{-1}, respectively).

Given the fact that steric factors played a dominant role in determining the relative strengths of ligand binding to the complexes **9** of

9
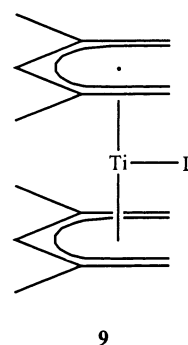
$Ti(2,4\text{-}C_7H_{11})_2$ [8], which is sterically less crowded than the $M(c\text{-}C_8H_{11})_2$ units, it is likely that steric factors also dominate here. However, there did appear to be some electronic preference for the $Ti(2,4\text{-}C_7H_{11})_2$ unit to be bound by accepting ligands, and thus there could be an accompanying electronic contribution favoring CO and cage phosphite coordination. In this regard, the C–O stretching frequencies for the $Ti(c\text{-}C_8H_{11})_2CO$ and $V(c\text{-}C_8H_{11})_2CO$ complexes are actually even lower than that in $V(C_5H_5)_2CO$ (1881 cm^{-1} [13]) whereas those for the
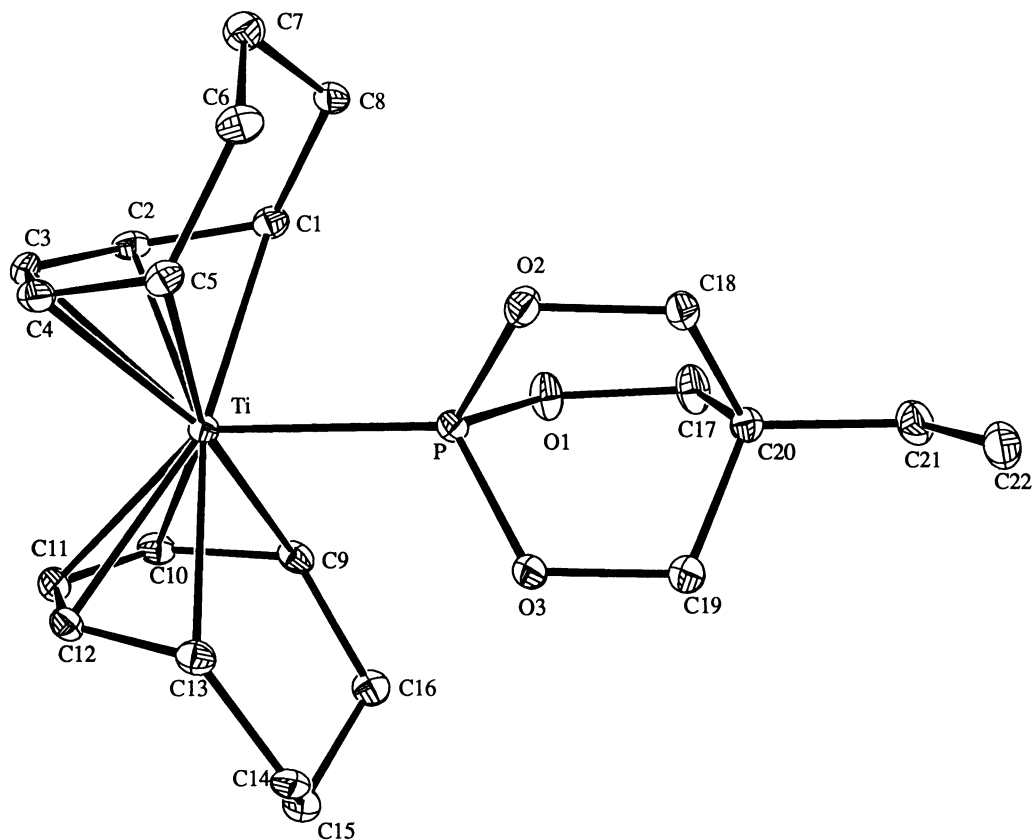
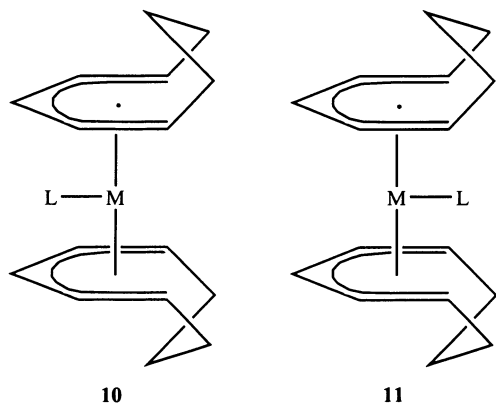Fig. 1. Solid state structure of Ti(c-C_8H_{11})$_2$[P(OCH$_2$)$_3$CEt].

respective M(6,6-dmch)$_2$CO (1904, 1912 cm^{-1}) and M(2,4-C$_7$H$_{11}$)$_2$CO (1952, 1948 cm^{-1}) complexes are significantly higher. Some, but not all [9d], of the decrease can be attributed to the electron donating effects of the carbon atoms attached to the terminal dienyl positions.

The ^{1}H- and ^{13}C-NMR spectra of the diamagnetic, 16 electron titanium complexes are indicative of a symmetric coordination geometry, as in **10** or **11**,

and in fact a structural determination of Ti(c-C$_8$H$_{11}$)$_2$(CO) revealed the geometry to be that of **11**, with the supplemental Lewis base coordination occur-

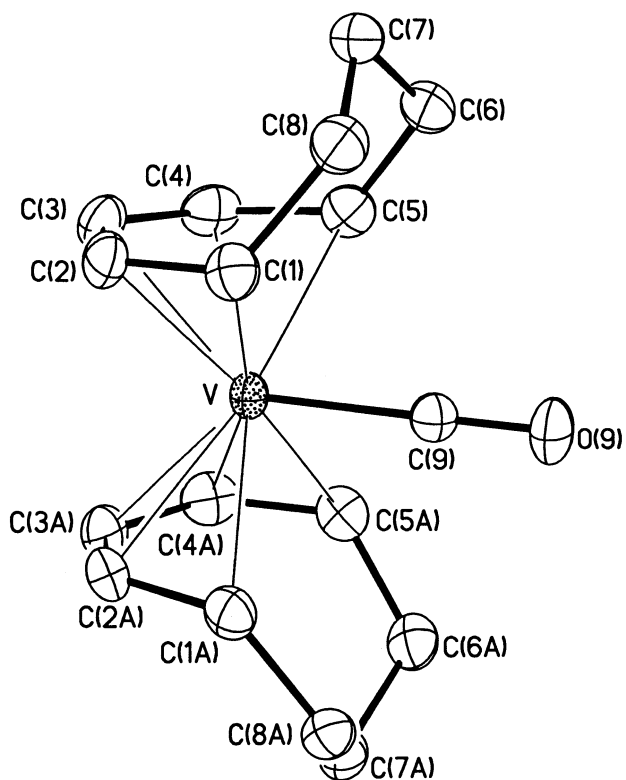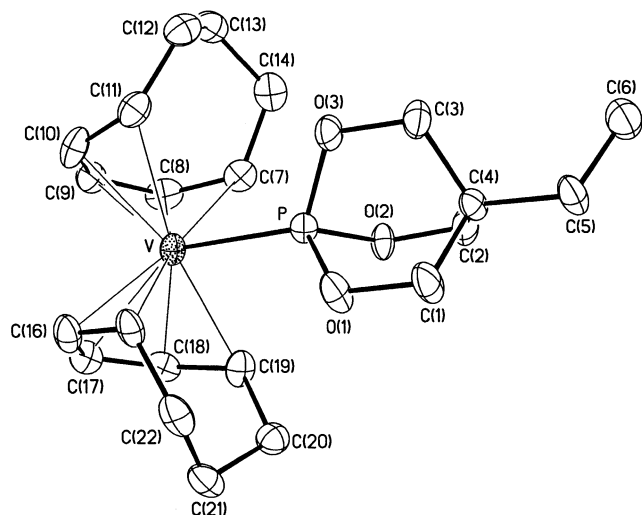Fig. 2. Solid state structure of V(c-C_8H_{11})$_2$(CO).

Fig. 3. Solid state structure of V(c-C$_8$H$_{11}$)$_2$[P(OCH$_2$)$_3$CEt].

Table 2
Pertinent bonding parameters for Ti(c-C$_8$H$_{11}$)$_2$[P(OCH$_2$)$_3$CC$_2$H$_5$]

Bond distances (Å)

Ti–C1	2.367(4)	Ti–C9	2.358(3)
Ti–C2	2.290(3)	Ti–C10	2.284(3)
Ti–C3	2.318(3)	Ti–C11	2.315(4)
Ti–C4	2.279(3)	Ti–C12	2.289(3)
Ti–C5	2.370(3)	Ti–C13	2.378(3)
C1–C2	1.418(5)	C9–C10	1.423(5)
C2–C3	1.420(5)	C10–C11	1.421(5)
C3–C4	1.424(5)	C11–C12	1.418(5)
C4–C5	1.422(5)	C12–C13	1.423(5)
Ti–P	2.434(1)	P–O2	1.629(3)
P–O1	1.631(2)	P–O3	1.623(2)

Bond angles (°)

C1–C2–C3	128.5(3)	C9–C10–C11	128.5(3)
C2–C3–C4	127.8(3)	C10–C11–C12	127.6(3)
C3–C4–C5	127.0(3)	C11–C12–C13	127.3(3)
Ti–P–O1	115.0(1)	Ti–P–O3	118.8(1)
Ti–P–O2	120.7(1)		

Table 3
Pertinent bonding parameters for V(c-C$_8$H$_{11}$)$_2$(CO)

Bond distances (Å)

V–C1	2.303(2)	C1–C2	1.411(2)
V–C2	2.211(2)	C1–C8	1.509(2)
V–C3	2.242(2)	C2–C3	1.414(3)
V–C4	2.214(2)	C3–C4	1.412(2)
V–C5	2.304(2)	C4–C5	1.418(2)
V–C9	1.904(2)	C5–C6	1.507(3)
C9–O9	1.156(2)	C6–C7	1.510(3)
		C7–C8	1.507(3)

Bond angles (°)

V–C9–O9	179.5(2)	C4–C5–C6	125.7(2)
C1–C2–C3	127.7(2)	C5–C6–C7	116.6(2)
C2–C3–C4	127.7(1)	C6–C7–C8	113.2(2)
C3–C4–C5	128.1(2)	C7–C8–C1	117.1(2)
		C8–C1–C2	125.4(2)

Table 4
Pertinent bonding parameters for V(c-C$_8$H$_{11}$)$_2$[P(OCH$_2$)$_3$CEt]

Bond distances (Å)

V–C7	2.325(6)	V′–C7′	2.394(6)
V–C8	2.328(5)	V′–C8′	2.247(6)
V–C9	2.264(6)	V′–C9′	2.259(6)
V–C10	2.232(6)	V′–C10′	2.201(6)
V–C11	2.380(7)	V′–C11′	2.296(7)
V–C15	2.324(6)	V′–C15′	2.297(7)
V–C16	2.237(6)	V′–C16′	2.202(6)
V–C17	2.258(6)	V′–C17′	2.265(6)
V–C18	2.212(6)	V′–C18′	2.201(6)
V–C19	2.273(7)	V′–C19′	2.257(6)
C7–C8	1.405(7)	C7′–C8′	1.414(7)
C8–C9	1.409(7)	C8′–C9′	1.386(8)
C9–C10	1.405(7)	C9′–C10′	1.381(8)
C10–C11	1.399(7)	C10′–C11′	1.404(8)
C15–C16	1.428(7)	C15′–C16′	1.394(7)
C16–C17	1.405(7)	C16′–C17′	1.415(7)
C17–C18	1.412(7)	C17′–C18′	1.410(7)
C18–C19	1.387(7)	C18′–C19′	1.416(7)
V–P	2.342(2)	V′–P′	2.361(2)
P–O1	1.626(4)	P′–O1′	1.612(4)
P–O2	1.633(4)	P′–O2′	1.619(4)
P–O3	1.619(4)	P′–O3′	1.612(4)

Bond angles (°)

C7–C8–C9	127.4(6)	C7′–C8′–C9′	128.0(7)
C8–C9–C10	127.8(6)	C8′–C9′–C10′	128.5(6)
C9–C10–C11	127.3(6)	C9′–C10′–C11′	128.7(7)
C15–C16–C17	127.0(6)	C15′–C16′–C17′	127.9(6)
C16–C17–C18	127.2(6)	C16′–C17′–C18′	125.5(6)
C17–C18–C19	126.9(6)	C17′–C18′–C19′	128.3(6)
V–P–O1	118.9(2)	V′–P′–O1′	118.8(2)
V–P–O2	116.0(2)	V′–P′–O2′	120.7(2)
V–P–O3	120.8(2)	V′–P′–O3′	116.2(2)

Table 5
Comparisons of averaged structural parameters (distances in Å, angles in °) for the M(c-C$_8$H$_{11}$)$_2$(L) complexes

| Parameter	Ti[P]	Ti(CO) [a]	V(CO)	V[P]
M–L	2.4345(10)	1.979(5)	1.904(2)	2.342(2)
M–C[1,5]	2.368(2)	2.363(3)	2.304(1)	2.318 [b]
M–C[2,4]	2.285(2)	2.265(3)	2.212(1)	2.230(4)
M–C[3]	2.316(2)	2.286(4)	2.242(2)	2.261(4)
M–C(avg.)	2.324	2.308	2.255	2.275
C[1]–C[2]–C[3]	127.8(2)	128.4(2)	127.9(1)	127.1(4)
C[2]–C[3]–C[4]	127.7(2)	128.5(3)	127.7(1)	127.5(4)
C[6,8] tilts [c]	62.9 (52.7)	59.3 (48.5)	61.0 (50.2)	63.1 (54.5)

[a] Reference [5].
[b] The individual values vary significantly due to steric interactions with the phosphite ligand.
[c] The first tilt angle is derived from torsion angles, while the sine of the second angle is derived from the ratio of the deviation of C6 or C8 from the ligand plane divided by the appropriate C–C[6 or 8] distance.

ring by the edge-bridges. While this is opposite to what is observed in edge-bridged half-open metallocenes, e.g. **8**, the preference of **11** compared with **10** can be attributed to the fact that in **10** one would have severe

interactions between the donor center and the central carbon atoms of the two dienyl fragments. The signals in the NMR spectra of the phosphite complex are quite broad at room temperature, indicative of partial dissociation of the Lewis base.

For the 17 electron $V(c\text{-}C_8H_{11})_2(L)$ (L = CO, $P(OCH_2)_3CEt)$ complexes, ESR spectra were readily obtained, and revealed vanadium hyperfine splittings of 76.6 G. This value is relatively similar to those of non-edge-bridged analogues, such as $V(C_5H_7)_2(CO)$ (79.1 Hz) [9,14], but markedly larger than observed for cyclopentadienyl (Cp) analogues [14,15]. For the cage phosphite complex, a phosphorus hyperfine splitting of 32.1 G was observed, somewhat smaller than found for $V(C_5H_7)_2P(OMe)_3$ ($A_V = 78$ Hz, $A_P = 38.7$ Hz).

The solid state structure of $Ti(c\text{-}C_8H_{11})_2(CO)$ has already been reported [5], and we now report also the structures of the related $M(c\text{-}C_8H_{11})_2(L)$ (M = Ti, L = $P(OCH_2)_3CEt$; M = V, L = CO, $P(OCH_2)_3CEt$) species for comparison. The structures of these species are shown in Figs. 1–3, and pertinent bonding parameters are provided in Tables 2–4. Table 5 contains a comparison of selected bonding parameters for these complexes. For the purposes of discussion, the M–C bonding parameters will be averaged assuming local C_{2v} symmetry for the dienyl portions of the $M(c\text{-}C_8H_{11})_2$ units (below).
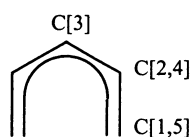

The structures of each of these species can be seen to conform to that of $Ti(c\text{-}C_8H_{11})_2(CO)$ (i.e. 11) or Wolczanski's related $Ti(6,6\text{-dmch})_2CO$ [4]. Before comparing the parameters of these species to each other, it is worth making some observations relative to the base free $M(c\text{-}C_8H_{11})_2$ species. Coordination by either CO or the phosphite leads to at most rather small increases in the M–C[3] and M–C[2,4] distances (≤ 0.02 and 0.04 Å, respectively). However, the M–C[1,5] distances respond dramatically, undergoing increases of ca. 0.12–0.15 Å, thereby changing from the shortest to the longest M–C(C_8H_{11}) bonds. These comparisons indicate that the ligand coordination leads to a displacement of the metal center more toward the central carbon atoms of the dienyl ligands, together with tilting between the dienyl ligands that serves to separate the terminal dienyl carbon atoms from the additional ligand, thereby leading to a relatively small separation between the central dienyl carbon atoms, e.g. an average of 3.05 Å for the vanadium phosphite compound. For the CO complexes, the tilts are fairly small (2–3°), but for the larger phosphite complexes, the tilts are substantially larger (ca. 12°).

From the data in Table 5, one can observe that the Ti–P, Ti–CO, and Ti–C(C_8H_{11}) distances are longer than their vanadium counterparts by 0.09, 0.075, and 0.05 Å, respectively. Similar trends exist for non-edge-bridged analogues [9]. Perhaps as a result of their steric demands, the pentadienyl ligands do not seem able to respond fully to the change in metal ion size [16], although there could also be a change in favorability of the bonding for the given ligand types as a result of the changes in metal ion size and d electron configuration.

Of the various types of M–C(C_8H_{11}) interactions, those for the formally uncharged carbon atoms in the 2 and 4 positions are consistently shortest, with those for the terminal (1,5) positions being longest. As noted above, in the absence of a supplemental ligand, the (Ti or V)–C[1,5] distances had been shortest. However, theoretical studies on other metal pentadienyl complexes have indicated that the relative M–C distances may not reflect the actual bonding favorabilities [17], and any interpretations regarding changes in actual bond strengths must be made with caution.

Further insight into the extent of steric crowding induced by the additional ligand coordination may be obtained by an examination of the distortions the dienyl ligands undergo from planarity. In each case the central carbon atoms, each directed toward its counterpart in the other dienyl ligand, lie substantially out of the dienyl plane (see Pictogram). The extent of these displacements can be gauged from the angles between the C[2,3,4] and C[1,2,4,5] planes. For the titanium and vanadium carbonyl complexes, these angles are 8.3 and 8.8°, while for the phosphite complexes the values are 8.5 and 10.3°, respectively. Further indication of the steric crowding is provided from the out-of-plane tilts by the C[6,8] substituents (Table 5). In the $M(c\text{-}C_8H_{11})_2$ complexes of titanium and vanadium, these tilts are approximately 46° (from least-squares plane data). The value for $Ti(c\text{-}C_8H_{11})_2(CO)$ is slightly greater, at 48.5°, reflecting relatively little effect. This is not surprising, given that one has the larger metal center together with the smaller additional ligand—the least crowded combination. However, the tilt increases to 50.2° for $V(c\text{-}C_8H_{11})_2(CO)$, and to ca. 53–55° for the phosphite complexes. For the vanadium phosphite complex, the V–C[1,5] distances are not very regular, providing further support for the expectation of especially severe steric problems in the complex.

In contrast to the C[6,8] tilts, all other substituents experience tilts *toward* the metal center. These tilts have been observed for both metal–pentadienyl [1] and metal–Cp [18] complexes, and attributed to an attempt to point the ligand π orbitals more toward the metal center, as in 12. For the titanium phosphite complex, the appropriate hydrogen atom
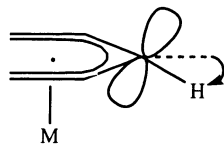
12

positions could be refined, and exhibited average tilts of 22.6, 20.0, and 4.6°, respectively, for the H[1,5], H[2,4], and H[3] substituents. It is, in fact, typical that the tilts for the H[1,5] positions will be greatest, and those for H[3] the least. The magnitude of tilting by H[2,4] seems greater than usual for normal pentadienyl ligands, but seems characteristic of larger ring edge-bridged dienyl ligands [5].

Some final comparisons may be made between Ti(c-C_8H_{11})$_2$(CO) and its smaller ring analogue, Ti(6,6-dmch)$_2$(CO) (dmch = dimethylcyclohexadienyl) [4]. In this species one also observes that the Ti–C[1,5] distances are substantially longer than the others, and that there is a significant tilt of ca. 28° between the two dienyl ligand planes. This tilt is much greater than the 2° tilt in Ti(c-C_8H_{11})$_2$(CO), clearly the result of the former's steric interactions between the dmch methyl groups and the CO ligand. The single carbon bridge in the dmch complex naturally leads to a much shorter C[1]–C[5] separation, ca. 2.407 versus 3.164 Å in Ti(c-C_8H_{11})$_2$(CO), as well as to a longer Ti-dienyl ligand plane separation, 1.912 versus 1.682 Å, and to smaller dienyl C–C–C angles, 119.4(8) versus 128.4(2)°.

In accord with previous studies, the presence of a bridge across the electronically open edge of a pentadienyl ligand leads to greatly enhanced steric crowding, as evidenced by the differences in some of their structural arrangements [11,19], by the dramatically weaker binding by additional ligands in edge-bridged open metallocenes, and by the substantial geometric distortions observed in such complexes. Additionally, the edge-bridges render the dienyl ligands better donors than typical pentadienyl ligands, and reasonably comparable to C_5H_5. For these, and perhaps other reasons, the edge-bridged complexes have been found to exhibit rather unique chemistry as compared with their non-bridged analogues [20], and these aspects are under continuing study.

4. Supplementary material

Crystallographic data for the structural analysis have been deposited with the Cambridge Crystallographic Data Centre, CCDC nos. 182524–182526 for the vanadium phosphite, vanadium carbonyl, and titanium phosphite complexes, respectively. Copies of this information may be obtained free of charge from The

Director, CCDC, 12 Union Road, Cambridge, CB2 1EZ UK (Fax: +44-1223-336033; e-mail: deposit@ccdc.cam.ac.uk or www: http://www.ccdc.cam.ac.uk).

References

[1] (a) R.D. Ernst, Chem. Rev. 88 (1988) 1255;
(b) R.D. Ernst, Comments Inorg. Chem. 21 (1999) 285.
[2] J.F. Helling, D.M. Braitsch, J. Am. Chem. Soc. 92 (1970) 7207, 7209.
[3] D.R. Wilson, A.A. DiLullo, R.D. Ernst, J. Am. Chem. Soc. 102 (1980) 5928.
[4] P.T. DiMauro, P.T. Wolczanski, Organometallics 6 (1987) 1947.
[5] V. Kulsomphob, R. Tomaszewski, G.P.A. Yap, L.M. Liable-Sands, A.L. Rheingold, R.D. Ernst, J. Chem. Soc. Dalton Trans. (1999) 3995.
[6] T.D. Newbound, L. Stahl, M.L. Ziegler, R.D. Ernst, Organometallics 9 (1990) 2962.
[7] R.D. Ernst, J.-Z. Liu, D.R. Wilson, J. Organomet. Chem. 250 (1983) 257.
[8] L. Stahl, R.D. Ernst, J. Am. Chem. Soc. 109 (1987) 5673.
[9] (a) R.D. Ernst, J.W. Freeman, L. Stahl, D.R. Wilson, A.M. Arif, B. Nuber, M.L. Ziegler, J. Am. Chem. Soc. 117 (1995) 5075;
(b) L. Stahl, W. Trakarnpruk, J.W. Freeman, A.M. Arif, R.D. Ernst, Inorg. Chem. 34 (1995) 1810;
(c) D. Vos, A.M. Arif, R.D. Ernst, J. Organomet. Chem. 553 (1998) 277;
(d) T.D. Newbound, A.L. Rheingold, R.D. Ernst, Organometallics 11 (1992) 1693.
[10] (a) I. Hyla-Kryspin, T.E. Waldman, E. Meléndez, W. Trakarnpruk, A.M. Arif, M.L. Ziegler, R.D. Ernst, R. Gleiter, Organometallics 11 (1992) 3201;
(b) R.W. Gedridge, J.P. Hutchinson, A.L. Rheingold, R.D. Ernst, Organometallics 12 (1993) 1553;
(c) R. Tomaszewski, K.-C. Lam, A.L. Rheingold, R.D. Ernst, Organometallics 18 (1999) 4174;
(d) W.-Q. Weng, A.M. Arif, R.D. Ernst, Organometallics 17 (1998) 4240.
[11] A.M. Wilson, F.G. West, A.L. Rheingold, R.D. Ernst, Inorg. Chim. Acta 300–302 (2000) 65.
[12] R. Tomaszewski, V. Kulsomphob, R.D. Ernst, unpublished results.
[13] F. Calderazzo, G. Fachinetti, C. Floriani, J. Am. Chem. Soc. 96 (1974) 3695.
[14] R.M. Kowaleski, F. Basolo, J.H. Osborne, W.C. Trogler, Organometallics 7 (1988) 1425.
[15] J.W. Freeman, N.C. Hallinan, A.M. Arif, R.W. Gedridge, R.D. Ernst, F. Basolo, J. Am. Chem. Soc. 113 (1991) 6509.
[16] R.D. Shannon, Acta Crystallogr. Sect. A 32 (1976) 751.
[17] M.C. Böhm, M. Eckert-Maksić, R.D. Ernst, D.R. Wilson, R. Gleiter, J. Am. Chem. Soc. 104 (1982) 2699.
[18] (a) M. Elian, M.M.L. Chen, D.M.P. Mingos, R. Hoffmann, Inorg. Chem. 15 (1976) 1148;
(b) A. Haaland, Acc. Chem. Res. 12 (1979) 415.

[19] B.G. Harvey, A.M. Arif, R.D. Ernst, unpublished results.
[20] (a) A.M. Wilson, F.G. West, A.M. Arif, R.D. Ernst, J. Am. Chem. Soc. 117 (1995) 8490;
  (b) R. Tomaszewski, I. Hyla-Kryspin, C.L. Mayne, A.M. Arif, R. Gleiter, R.D. Ernst, J. Am. Chem. Soc. 120 (1998) 2959;
  (c) R. Basta, R.D. Ernst, unpublished results;
  (d) V. Kulsomphob, B.G. Harvey, A.M. Arif, R.D. Ernst, Inorg. Chim. Acta, 334 (2002) 17.